

Electron Backscatter Diffraction Analysis of the Microstructure Fineness in Pure Copper under Torsional Deformation

C. P. Wang,^a J. K. Fan,^{b,1} F. G. Li,^c and J. C. Liu^{a,2}

^a School of Materials Science and Engineering, Tianjin Polytechnic University, Tianjin, China

^b School of Mechanical and Power Engineering, Henan Polytechnic University, Jiaozuo, China

^c School of Materials Science and Engineering, Northwestern Polytechnical University, Xi'an, China

¹ junkaifan@163.com

² jchliu@tjpu.edu.cn

Torsional deformation is regarded a promising deformation procedure to prepare the gradient structural materials. Pure copper was subjected to large plastic strains in torsion. Electron backscatter diffraction analysis was used to explore the microstructure evolution. The observations demonstrate that both high-angle grain boundaries and misorientation increase with strain. The grains finer and more homogeneous. In addition, the microstructure within the shear band demonstrates a distinct preferred orientation. The crystal $\langle 110 \rangle$ direction is parallel to the shear direction, and the crystal $\{111\}$ inclines to the plane shear surface. A torsion-induced bar specimen includes a $\{011\} \langle 211 \rangle$ brass texture, $\{011\} \langle 100 \rangle$ Gaussian texture, and stronger $\{112\} \langle 111 \rangle$ copper texture.

Keywords: severe plastic deformation, copper, torsion, microstructure, texture.

Introduction. Gradient structural metal materials exhibit many enhanced properties, which imply higher strength, plasticity, hardness, and lower wear and alloying [1], etc. Torsional deformation can be utilized to fabricate materials with a gradient structure, improve their mechanical properties, and reduce the anisotropy [2–6]. Therefore, such deformation can be used to prepare gradient structural materials. Furthermore, torsional deformation is recognized to be a kind of severe plastic deformation (SPD) method to obtain a higher plasticity strain than that in tension or compression [7]. As a representative example of SPD methods, high-pressure torsion (HPT) has an apparent and unique advantage in producing ultrafine-grained (UFG) materials with superior mechanical properties due to employing a superior compressive and torsional deformation into the materials [7]. The torsion study is noticeable in the probe of SPD deformation behavior. Over the last century, the study on the torsion was intense for the basic mechanics research [8–11]. However, to date, limited work referring to the torsion is available. Thus, it is expedient to investigate the microstructure evolution of torsion-deformed copper via the electron backscatter diffraction (EBSD) analyses.

1. Experimental Procedures. The starting bars of commercial pure copper bars (99.7 in wt.%) had a fully re-crystallized microstructure with the grain size ranging from about 20 to 40 μm . The initial bars were machined into torsional specimens with dimensions of 35 mm in gauge length and 5 mm in diameter (Fig. 1a), and torsional deformation was applied to achieve high strains. The torsional deformation was applied using a wire torsion-testing machine XC-10 under the torsional rate of 30 rpm. All the experimental procedures followed the National Standard of China GB/T 10128-2007. Three specimens were deformed in torsion at room temperature by rotations of 3.86, 11.58, and 19.30 turns, corresponding to the maximum equivalent strains of 1, 3, and 5 at the specimen surface, respectively. Figure 1b shows the photograph of torsional specimens. The equivalent strain in torsion can be calculated by following equations [12]:

$$\gamma = 2\pi Nr/L, \quad \varepsilon = \gamma/\sqrt{3},$$

where ε is equivalent strain, γ is shear strain, N is the number of rotation, r is radial position of the specimen, and L is gauge length of the specimen.

The received torsional specimens for EBSD were sectioned to analyze the microstructure. The EBSD scans were carried out in the longitudinal section at $r = 0.9R$, where R is the specimen radial position from its center (Fig. 1c). Specimens for EBSD analysis were prepared by mechanical polishing following standard metallographic procedures. EBSD observation was carried out in JEOL JSM-7001 F Field Emission SEM (at 20 kV accelerate voltage) using the Oxford Instruments HKL Channel 5 software package. For more detailed structure reconstruction, a half width was 10° , and the cluster size was 5° . The textures are represented in the TD-ND-ED reference system (Fig. 1c).

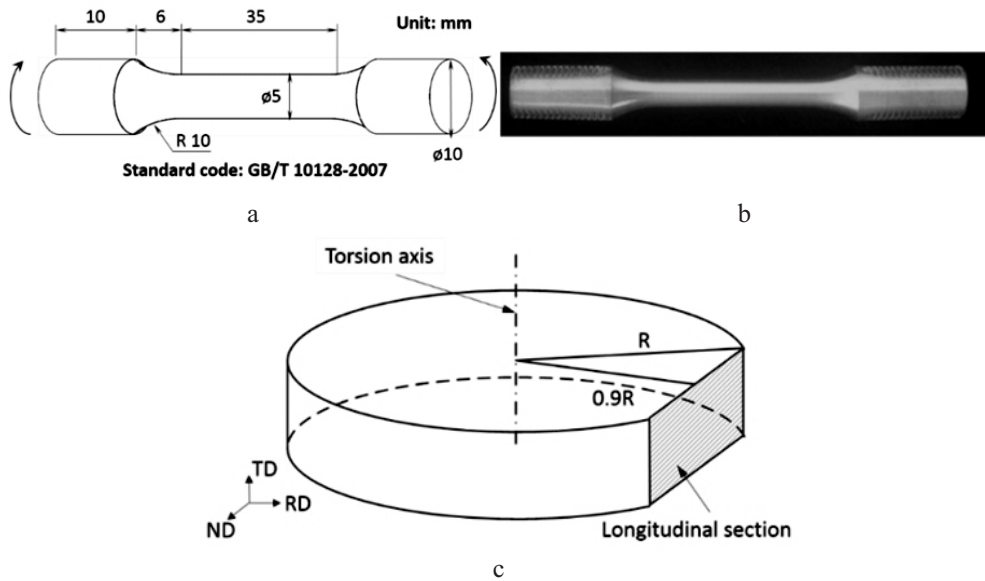


Fig. 1. Schematic illustrations of (a) different reversal torsion processes, (b) photograph of pre-torsion deformed specimens, and (c) measured positions.

2. Results and Discussion. The grain size and misorientation angle distributions of pure copper formed by different torsional processes with low strains are shown in Fig. 2a and 2b. The coarse grain is elongated and the microstructure has an obvious shear band texture. With an increase in the torsional strain, the dislocation cell emerges in $\varepsilon = 3$. In the SPD induced material, with the increase of strain, the microstructure of band shear continuously gathers a large number of dislocations, and the dislocation tangles form the dislocation cells [4]. For the morphology of $\varepsilon = 5$, the obvious equiaxed grains emerge. The grain boundaries of subgrains and fine-grains become straight and clearly visible, at the bottom of figure. Figure 2b shows the distribution of grain size calculated according to the EBSD grain map. With an increase in the torsion strain, the average grain size becomes smaller, and the area fraction shifts from the large local area of $\sim 40 \mu\text{m}$ into small local area of $\sim 10 \mu\text{m}$.

The grain boundary distribution of pure copper subjected by different torsion strains is constructed, as shown in Fig. 2a and 2c. The grain boundary of random low angle is labeled with black thin lines, and the grain boundary of low angle greater than 10° is labeled with bold red lines. The counterpart of less than 2° has been removed. In the low torsional strain,

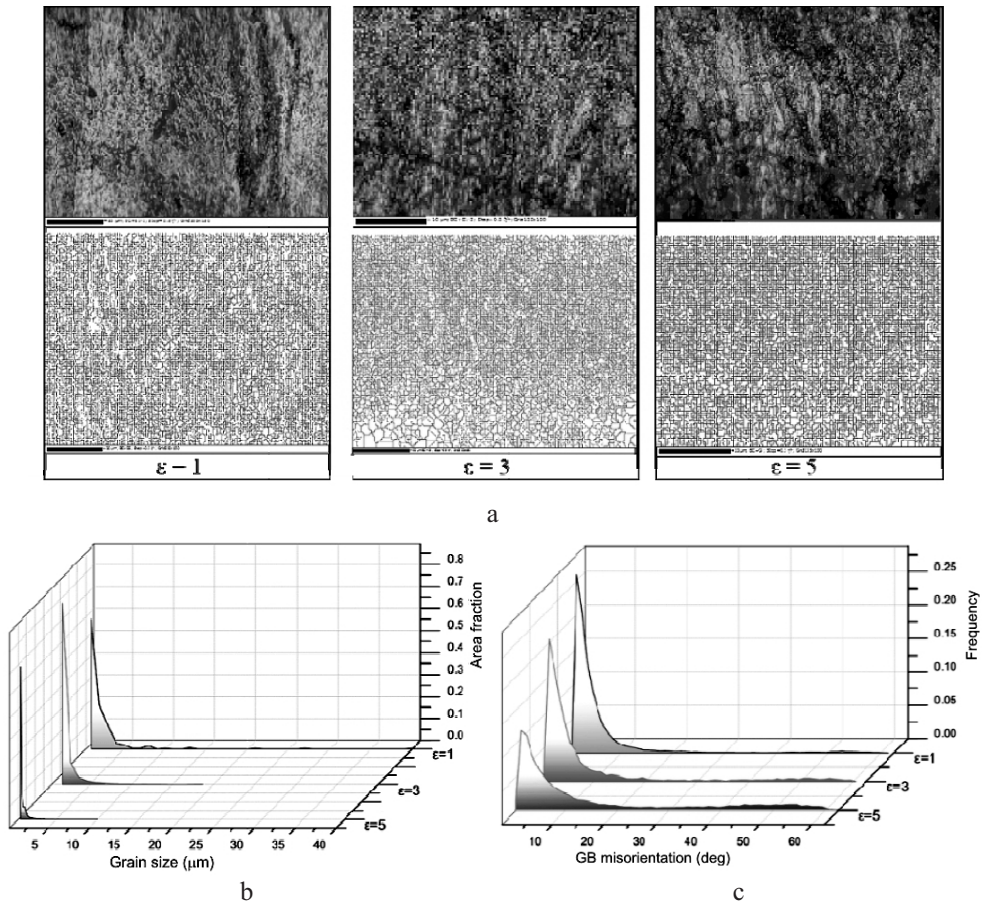


Fig. 2. Microstructural characteristics of pure copper after different torsion process. (a) distributions of grain and grain boundary, statistical fraction of (b) grain size and (c) misorientation angle.

the low angle grain boundaries are the majority. The subgrain boundaries have been transformed into the high angle grain boundaries (HAGBs), and the fine grains tend to be clustered together to form a chain network structure ($\epsilon = 3$). The red lines of $\epsilon = 3$ are denser than those of $\epsilon = 5$ due to the high dislocation density and numerous dislocation cells. The low angle grain boundaries (LAGBs) decrease and the proportion of fine grains increases significantly with the strain increasing. Similar phenomena are also found in purity aluminum heavily deformed by torsion [13].

Figure 3 represents the $\{111\}$ incomplete pole figures (PFs) of pure copper in $\epsilon = 1, 3,$ and 5 of torsion. As shown in figures, the strong preferred orientation forms in the PFs. The density of 18.77, 5.55, and 6.30 are for $\epsilon = 1, 3, 5$. The orientation and intensity of three kinds of texture are obviously different due to the dynamic formation of texture during torsion. The intensity and direction are closely related to the strain state of deformed materials. Moreover, the orientation tends to be $\{112\}$. The new texture is related to the segregation direction of a certain crystal group under the external force. The original state of aggregation is destroyed in the process of internal stress transferring into the adjacent gain boundary.

Figure 4 demonstrates the inverse pole figures (IPFs) on RD direction of the specimens deformed by torsional strain of $\epsilon = 1, 3,$ and 5. As can be seen from figures, the torsion specimen under a small amount of deformation is the main $\langle 110 \rangle$ fiber texture.

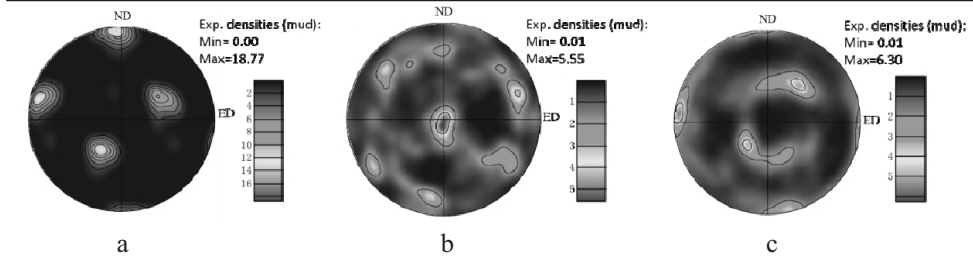


Fig. 3. PFs of pure copper processed by torsion strain. Here and in Figs. 4 and 5: (a) $\varepsilon = 1$; (b) $\varepsilon = 3$; (c) $\varepsilon = 5$.

With an increase in torsion strain, the $\langle 110 \rangle$ crystal orientation dominates in the $\langle 111 \rangle$ direction, accompanied with a slight accumulation of $\langle 001 \rangle$ crystal orientation. Moreover, the lattice distortion is more obvious, and the concentration trends to the $\langle 111 \rangle$ orientation. Bhattacharyya et al. [12] found that the pure copper was in the shear deformation of high strain rate, and the crystal $\langle 110 \rangle$ direction tended to the texture characteristics of shear direction. In the deformation process of pure copper, the main slip system is $\{111\} \langle 110 \rangle$. The sliding direction of crystal tends to be in the shear direction, and the sliding plane tends to the shear plane.

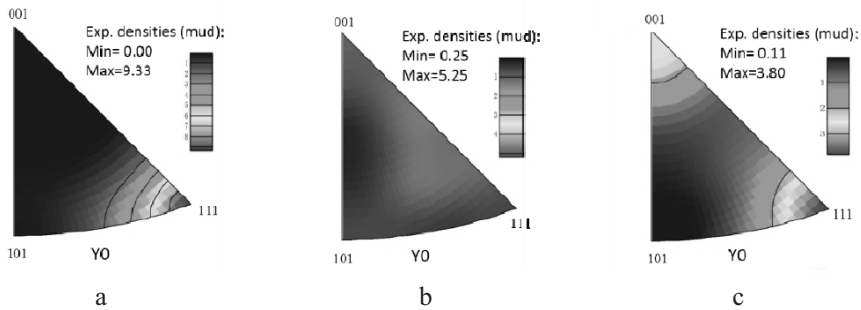
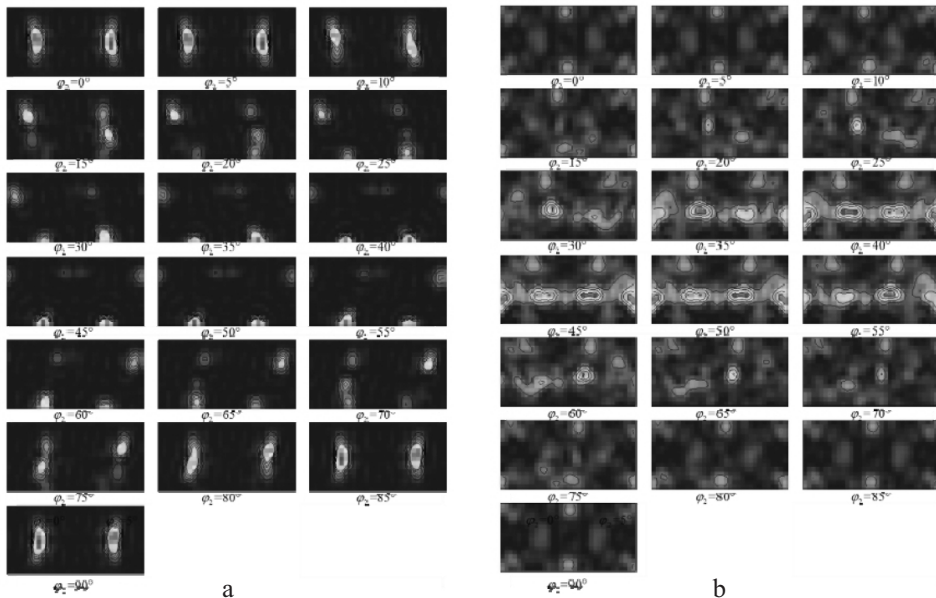


Fig. 4. IPFs of copper subjected to torsional strain.



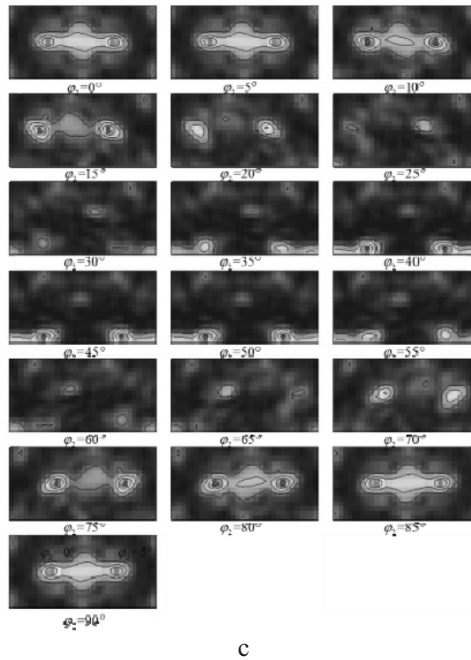


Fig. 5. ODF diagrams of pure copper subjected to torsional strain.

The orientation distribution function (ODF) diagrams calculated from EBSD data are illustrated in Fig. 5. The obvious $\{011\} \langle 211 \rangle$ brass type texture and $\{011\} \langle 100 \rangle$ Gaussian texture indicate that the $\{110\}$ plane of all orientations is parallel to the torsional shear direction, and the Gaussian orientation is the shear texture of pure copper. Additionally, the strong $\{112\} \langle 111 \rangle$ copper type texture is due to the material strain.

Conclusions

1. The misorientation angle of grain boundary increases with the torsional strain. The number of HAGBs also increases. The grains are finer and more homogenous in the torsion-induced copper, and gradually transforms into a granular structure with HAGBs.

2. The microstructure exhibited an obvious preferred orientation inside the shear zones. The texture is mainly $\langle 110 \rangle$ fiber texture for low strain, and the $\langle 111 \rangle \langle 110 \rangle$ crystal orientation for high strain, accompanied with a slight $\langle 001 \rangle$ crystal orientation.

3. With an increase in the torsional strain, the textures of torsional specimens are mainly $\{011\} \langle 211 \rangle$ type brass and $\{011\} \langle 100 \rangle$ Gaussian type, as well as $\{112\} \langle 111 \rangle$ copper textures.

Acknowledgments. This work was partially supported by National Natural Science Foundation of China (No. 51275414, No. 51172161, No. 51405136, and No. 51505191), School Youth Foundation (No. 1205-04020202), the fund of the State Key Laboratory of Solidification Processing in NWPU (No. SKLSP201517), and Doctor Foundation of Henan Polytechnic University (No. B2015-37).

1. T. H. Fang, W. L. Li, N. R. Tao, and K. Lu, "Revealing extraordinary intrinsic tensile plasticity in gradient nano-grained copper," *Science*, **331**, No. 6024, 1587–1590 (2011).

2. J. Wang, D. Zhang, Y. Li, et al., "Effect of initial orientation on the microstructure and mechanical properties of textured AZ31 Mg alloy during torsion and annealing," *Mater. Design*, **86**, 526–535 (2015).
3. N. Guo, B. Song, H. Yu, et al., "Enhancing tensile strength of Cu by introducing gradient microstructures via a simple torsional deformation," *Mater. Design*, **90**, 545–550 (2016).
4. C. Wang, F. G. Li, J. Li, et al., "Microstructure evolution, hardening and thermal behavior of commercially pure copper subjected to torsional deformation," *Mater. Sci. Eng. A*, **598**, 7–14 (2014).
5. J. H. Li, F. G. Li, M. Z. Hussain, et al., "Micro-structural evolution subjected to combined tension–torsional deformation for pure copper," *Mater. Sci. Eng. A*, **610**, 181–187 (2014).
6. B. Song, N. Guo, R. Xin, et al., "Strengthening and toughening of extruded magnesium alloy rods by combining pre-torsional deformation with subsequent annealing," *Mater. Sci. Eng. A*, **650**, 300–304 (2016).
7. C. P. Wang, F. G. Li, L. Wei, et al., "Experimental microindentation of pure copper subjected to severe plastic deformation by combined tension–torsion," *Mater. Sci. Eng. A*, **571**, 95–102 (2013).
8. A. Nadai, *Theory of Flow and Fracture of Solids*, McGraw-Hill, New York (1950).
9. J. Chakrabarty, *Theory of Plasticity*, Butterworth-Heinemann, Oxford (2006).
10. Y. Estrin, L. S. Tóth, A. Molinari, and Y. Bréchet, "A dislocation-based model for all hardening stages in large strain deformation," *Acta Mater.*, **46**, No. 15, 5509–5522 (1998).
11. N. A. Fleck, H. M. Muller, M. F. Ashby, and J. W. Hutchinson, "Strain gradient plasticity: theory and experiment," *Acta Metall. Mater.*, **42**, No. 2, 475–487 (1994).
12. A. Bhattacharyya, D. Rittel, and G. Ravichandran, "Effect of strain rate on deformation texture in OFHC copper," *Scripta Mater.*, **52**, No. 7, 657–661 (2005).
13. S. Khamsuk, N. Park, H. Adachi, et al., "Evolution of ultrafine microstructures in commercial purity aluminum heavily deformed by torsion," *J. Mater. Sci.*, **47**, No. 22, 7841–7847 (2012).

Received 15. 09. 2017